Systematic Survey of the Correlation between Northern HECR Events and SDSS Galaxies

Hajime Takami[1], Takahiro Nishimichi[2], Katsuhiko Sato[1,3]

[1] Institute for the Physics and Mathematics of the Universe, the University of Tokyo, 5-1-5, Kashiwanoha, Kashiwa, Chiba 277-8568, Japan

[2] Department of Physics, the University of Tokyo, 7-3-1, Hongo, Bunkyo-ku, Tokyo 113-0033, Japan

[3] Department of Physics, School of Science and Engineering, Meisei University, 2-1-1, Hodokubo, Hino-shi, Tokyo 191-8506, Japan

E-mail: hajime.takami@ipmu.jp

Abstract. We find statistically significant spatial correlations between the arrival directions of the highest energy cosmic rays (HECRs) observed by the Akeno Giant Air Shower Array (AGASA) and large-scale structure of galaxies observed by Sloan Digital Sky Survey (SDSS) in the redshift ranges of $0.006 \leq z < 0.012$ and $0.012 \leq z < 0.018$ at angular scale within $\sim 5^\circ$. This result supports a hypothesis that the sources of HECRs are related to galaxy distribution even in the northern sky, which has been already indicated by Pierre Auger Observatory in the southern sky. We also investigate the dependency of the correlation on the absolute magnitude, color, and morphology of the galaxies. For galaxies with $0.006 \leq z < 0.012$, the correlation tends to be stronger for luminous and red galaxies. Based on these results, we discuss plausible HECR sources and constraint on Galactic magnetic field.

PACS numbers: 95.85.Ry,98.70.Sa

1. Introduction

Although the sources of the highest energy cosmic rays (HECRs) have been poorly known, recent observations begin to unveil a part of the nature of HECR origin. The first indication to HECR sources was reported by the Akeno Giant Air Shower Array (AGASA). The AGASA reported the anisotropic distribution of cosmic rays (CRs) above 4×10^{19} eV at small angular scale comparable with their angular uncertainty to determine arrival directions of primary CRs [1]. The anisotropic feature has been interpreted as the existence of point-like extragalactic sources. An important step to their origin is the positional correlation between the arrival directions of HECRs with energies above $\sim 6 \times 10^{19}$ eV and nearby astrophysical objects reported by the Pierre Auger Observatory (PAO) [2, 3]. These results strongly suggested that HECRs should be of extragalactic origin. Several groups have also analyzed the PAO data by using catalogs of different astrophysical objects and then have confirmed the correlation with matter (or galaxy) distribution of local Universe [4, 5, 6, 7]. Although the same analysis of new PAO data as Refs. [2, 3] shows the decreases of the significance level of the correlation [8], the correlation with the large-scale structure is still positive [9].

The PAO observes HECRs from the southern sky, since it is located in Argentina. If HECR sources are extragalactic objects as suggested by the PAO, the correlation of HECRs and galaxy distribution is also expected in the northern sky. However, such correlation has never been clearly reported, though the correlation of HECRs with the supergalactic plane was reported in the northern sky [10, 11]. We tested the correlation of the AGASA data with galaxies of Infrared Astronomical Satellite Point Source Redshift Survey (IRAS PSCz) [12], but a significantly positive correlation could not be found [7]. There are two reasons why we have not found such correlation when we assume that the correlation exists in the northern sky. One is the small exposure of the AGASA relative to the PAO. In the period of Refs. [2, 3], the total exposure of the PAO is ~ 7 times as large as that of the AGASA. Thus, the AGASA may not have the number of highest energy (HE) events large enough to find correlation. The other is the completeness of a galaxy catalog used in [7]. In other words, it is the possibility that the IRAS PSCz catalog of galaxies does not reflect the large-scale structure of galaxy distribution in local Universe.

In this study, we focus the latter reason, because the former problem cannot be solved by us without accumulating more number of HECR events. We investigate the correlation between HECR events observed in the northern sky and galaxy distribution which has higher completeness than the IRAS PSCz catalog. For this purpose, we adopt galaxies observed by Sloan Digital Sky Survey (SDSS) [13]. The SDSS is a survey project of galaxies to investigate the large-scale structure of the Universe in optical bands and therefore can observe faint galaxies down to $m_r \sim 20.0$ where m_r is the r-band apparent magnitude of galaxies. Thus, SDSS galaxies better trace the structure of the local Universe. As HECR events observed in the northern sky, we adopt the AGASA data published in Ref. [14].

This paper is laid out as follows: in Section 2, we explain the data samples of HECR events and galaxies in detail. Also, a statistical method which we adopt to test the correlation between them is described. In Section 3, we calculate cross-correlation functions defined in Section 2 between the AGASA events and SDSS galaxies with several redshift ranges. We also investigate the dependencies of the correlation on the r-band absolute magnitude, color, and morphology of galaxies. These give us useful information to search for the HECR sources because the features of the host galaxies reflect the nature of objects contained in the hosts. Section 4 is devoted to discuss and interpret the results obtained in Section 3. Finally, we conclude this study in Section 5.

2. Data Samples and Statistical Method

2.1. Sample of Highest Energy Cosmic Rays

We adopt the AGASA data published in Ref. [14] as a sample of HECR events observed in the northern hemisphere. We have two reasons why we use this sample: (i) that the AGASA data is the largest sample in the northern sky in which the energy and arrival direction of each event are published and (ii) the AGASA is a ground array whose directional dependence of the aperture is easier to estimate analytically than that of fluorescence telescopes like High Resolution Fly's Eye (HiRes).

That event sample consists of 57 events with energies above 4×10^{19} eV in the energy-scale of the AGASA, 8 events out of which are so-called *super-GZK* events [15] which mean that their energies are larger than the energy of a spectral cutoff ($\sim 10^{20}$ eV) predicted from interactions with cosmic microwave background (CMB) photons (Greisen-Zatsepin-Kuz'min (GZK) cutoff; [16, 17]). Since these super-GZK events are difficult to be simply produced by astrophysical scenarios, their origin have often been proposed in beyond standard model physics (for a review, see Ref. [18]). An astrophysical solution is the existence of their sources within several tens of Mpc which is comparable with the energy-loss length of photopion production of HECRs in CMB. Although the GZK steepening of HECR spectrum is not observed by the HiRes [19] and PAO [20] and is a problem itself, we simply assume that all events are of astrophysical origin in this study to use this sample and analyze them.

2.2. Sample of Galaxies

We use data from the 7th data release (DR7) of the SDSS [21], especially large-scale structure subsample named *dr72bright0* sample of the New York University Value Added Catalog (NYU-VAGC) [22]. This is a spectroscopic sample of galaxies with u,g,r,i,z-band (K-corrected) absolute magnitudes, r-band apparent magnitude m_r, redshifts, and information on the mask of the survey. Spectroscopic galaxies are selected by conditions of $10.0 \leq m_r \leq 17.6$ and $0.001 \leq z \leq 0.5$. Strictly speaking, the upper bound of apparent magnitude of galaxies is less than 17.6 in a very small fraction of regions, but

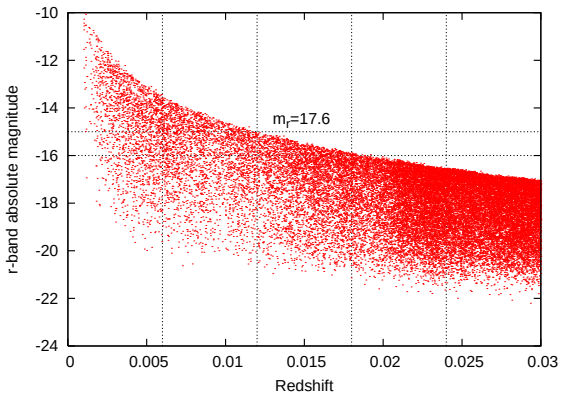

Figure 1. Redshift vs. r-band absolute magnitude of SDSS galaxies within $z = 0.03$.

we have practically no problem to regard the upper bound as 17.6 because the fraction of such regions is less than 0.1%.

We construct an approximately volume-limited sample of SDSS galaxies to analyze the cross-correlation between the AGASA events and galaxy distribution. Fig. 1 plots the r-band absolute magnitude of all the SDSS galaxies in the sample within $z \leq 0.03$ as a function of their redshifts. We can clearly see a line due to the flux limit determined by $m_r = 17.6$.

We study the cross-correlation with galaxies within $z = 0.024$ which corresponds to ~ 100 Mpc in the concordance cosmology. The GZK horizon of protons with the energy of $\sim 4 \times 10^{19}$ eV are larger than ~ 100 Mpc. Fig. 2 shows the cumulative fraction of the flux of protons arriving from sources with distances representing the horizontal axis to the total flux of protons. The left and right panels are for protons with energies of $10^{19.6}$ eV and $10^{19.8}$ eV, respectively. The cumulative fractions are calculated under several assumptions on the nature of HECR sources: a spectral index α and a cosmological evolution factor of HECR source density with a shape of $(1+z)^m$, the static emission of protons, and neglecting intergalactic magnetic field (IGMF). For these calculations, we assume a ΛCDM cosmology with $H_0 = 71$ km s^{-1} Mpc^{-1}, $\Omega_m = 0.3$, and $\Omega_\Lambda = 0.7$, as the Hubble parameter, the ratio of matter density to the critical density, and the ratio of cosmological constant to the critical density, respectively. We can see that the fraction of protons arriving at the Earth from sources within 100 Mpc is only 10-20 %. Even for protons with $10^{19.8}$ eV, the fraction is maximally ~ 40 %. However, IGMF could more deflect the trajectories of HECRs emitted from sources with larger distances and therefore the cross-correlation signal between arriving HECRs and such sources may be weaken. In the case of the PAO data, we cannot find any significant signal of positive correlation with a galaxy distribution with $z > 0.018$, whereas significantly positive correlation was found for $z \leq 0.018$ [7]. The angular scale of the positive correlation is up to $\sim 15^\circ$. These indicate a possibility that HECRs emitted from distant sources are significantly deflected by intervening magnetic fields. Therefore, it is natural to focus on the cross-correlation of UHECRs with nearby galaxy distribution in order to constrain

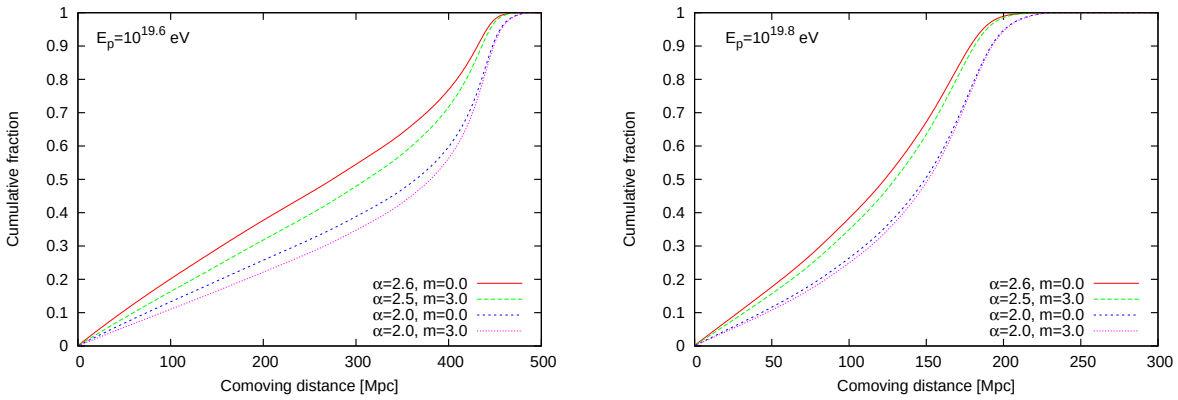

Figure 2. Cumulative ratios for sources to contribute to the fluxs of extragalactic protons with $10^{19.6}$ eV (*left*) and $10^{19.8}$ eV (*right*) at the Earth.

their sources.

In order to construct a volume-limited sample of galaxies, we consider galaxies with the absolute magnitude below -17 within $z = 0.024$. Under this criterion, all the galaxies with $M_r \leq -17$ within 100 Mpc are included in the galaxy sample, as we can see in Fig. 1.

2.3. Cross-correlation Function

We adopt a cross-correlation function used in our previous work [7], which was originally introduced in Ref. [23] for the cross-correlation between two types of galaxies,

$$w_{\rm eg}(\theta) = \frac{EG(\theta) - EG'(\theta) - E'G(\theta) + E'G'(\theta)}{E'G'(\theta)}. \quad (1)$$

E, G, E' and G' represent HECR events, galaxies in the catalog, HECR events randomly put with number density proportional to the detector aperture, and galaxies randomly put following the angular selection function (e.g., survey window, bright star mask, and so on) in the observed sky, respectively. $EG(\theta)$ is the number of pairs between E and G with the angular distance from θ to $\theta + \Delta\theta$ normalized by the number of HECR events multiplied by the number of galaxies. We set $\Delta\theta = 1^\circ$, which is comparable to the typical angular determination scale of the arrival directions of primary cosmic rays for HECR observatories. $EG'(\theta)$, $E'G(\theta)$, and $E'G'(\theta)$ are also defined similar to $EG(\theta)$. E' and G' enable us to correct the non-uniformities of the HECR aperture and the galaxy sampling.

The aperture of a ground array depends on the declination of observed directions reflecting the daily rotation of the Earth. The declination dependence of the exposure (= aperture $\times$ observation time) can be analytically estimated as [24]

$$\omega(\delta) \propto \cos(a_0)\cos(\delta)\sin(\alpha_m) + \alpha_m \sin(a_0)\sin(\delta), \quad (2)$$

where α_m is given by

$$\alpha_m = \begin{cases} 0 & \text{if } \xi > 1 \\ \pi & \text{if } \xi < -1 \\ \cos^{-1}(\xi) & \text{otherwise} \end{cases}, \tag{3}$$

and

$$\xi \equiv \frac{\cos(\theta) - \sin(a_0)\sin(\delta)}{\cos(a_0)\cos(\delta)}. \tag{4}$$

Here, a_0 is the terrestrial latitude of a ground array and θ is the zenith angle for a data cut because of experimental reasons. For the AGASA, $a_0 = 35°47'$ and $\theta = 45°$ [14]. We produced the E' sample in Eq. (1) following Eq. (2). We set the number of E' sample to be twenty times more than the actual HECR events.

The survey area of the SDSS is also limited and very complicated due to masks. The SDSS observes about one fifth of the whole sky and the depth of observations slightly depends on directions. We take account of these effects by distributing random galaxies (i.e., G' in Eq. 1) following the angular selection function. We use `mangle` software [25, 26] to do so. Again we distribute at least twenty times more random galaxies than the real ones, which is an usual choice, and then confirmed that this particular choice does not affect the results.

3. Results

This section is dedicated to show results of our analysis. First of all, we consider the cross-correlation between the AGASA events and SDSS galaxies in 4 ranges of redshifts within $z = 0.024$, which corresponds to ~ 100 Mpc in the concordance cosmology, in Section 3.1. This analysis will lead to a result that the AGASA events correlate more with SDSS galaxies in intermediate redshift ranges. Next, we focus on these galaxies and investigate the dependency of the cross-correlation on the absolute magnitude of the galaxies 3.2. Then, we also consider the dependencies of color and morphology of galaxies to find the nature of environment for HECR generation 3.3.

3.1. Dependence on Redshift

We divide our sample of galaxies into 4 parts in redshift for every 0.006, which corresponds to ~ 25 Mpc. Note that the flux of HECRs from sources in each shell is comparable if we assume that HECR composition is proton and IGMF is neglectable as we can see in Fig. 2, i.e., all the lines in Fig. 2 can be well approximated by straight lines within 100 Mpc. We consider the cross-correlations between the AGASA data and these 4 samples of galaxies. Results are shown in Fig. 3.

In the left panels, we show the positions of galaxies (*red dots*) and the arrival directions of the AGASA events with $E > 4 \times 10^{19}$ eV (*circles*) for 4 redshift ranges of galaxies: $0.001 \leq z < 0.006$, $0.006 \leq z < 0.012$, $0.012 \leq z < 0.018$, and $0.018 \leq z < 0.024$ from top to bottom, for visibility. The super-GZK events, which are

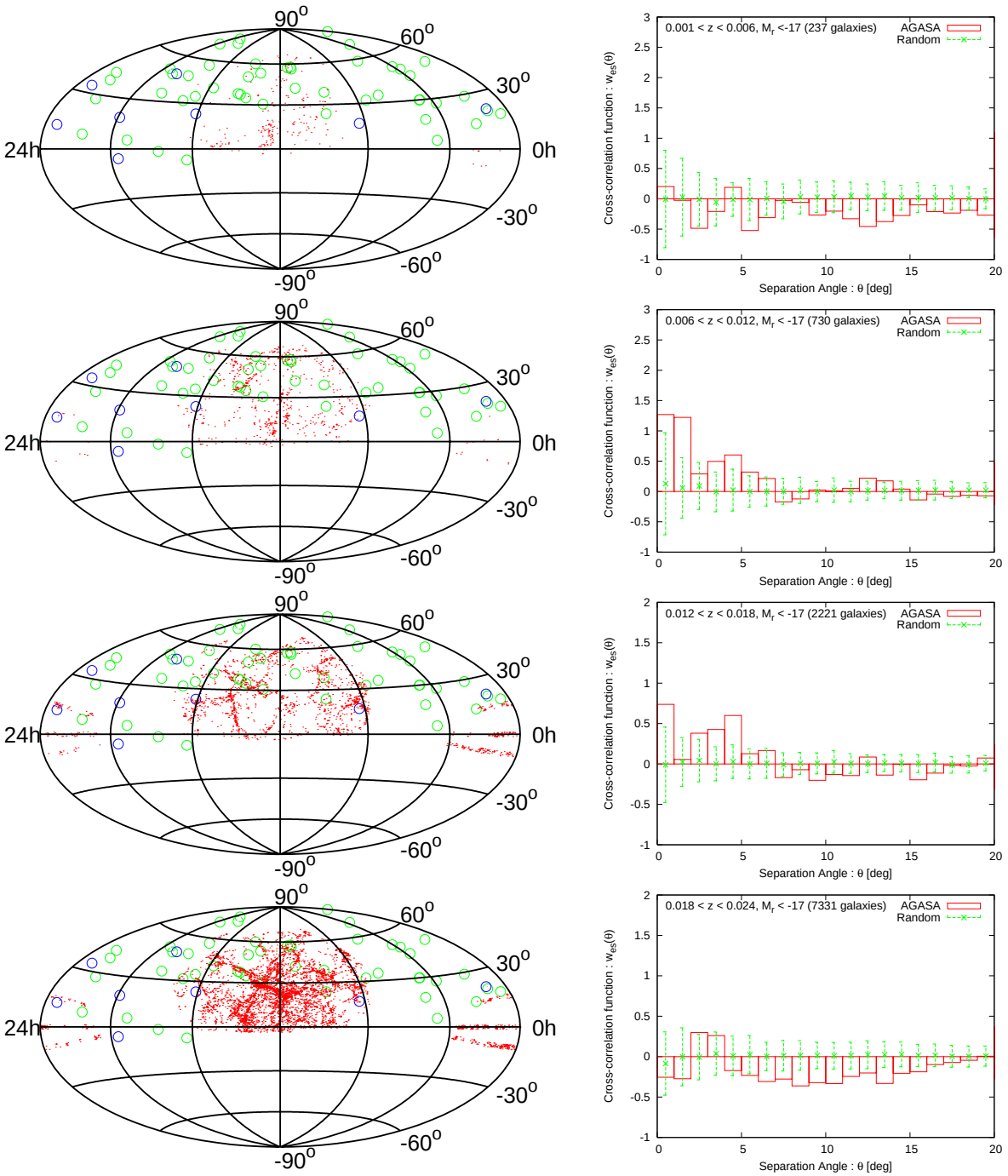

Figure 3. *left*: Skymaps of the AGASA events and SDSS galaxies with $M_r \leq -17$. The redshift ranges of SDSS galaxies (plotted in red) considered are $0 \leq z < 0.006$, $0.006 \leq z < 0.012$, $0.012 \leq z < 0.018$, and $0.018 \leq z < 0.024$ from top to bottom. The AGASA events are also ploted as circles ($E > 4 \times 10^{19}$ eV; green, $E > 10^{20}$ eV; blue). *right*: Cross-correlation functions between the AGASA events and SDSS galaxies calculated from the corresponding left panels (*histogram*). We also show the cross-correlation functions calculated from randomly distributed events in green.

Fig.	Redshift	Conditions	Number of galaxies
for Fig. 3	$0.001 \leq z < 0.006$	$M_r \leq -17$	237
	$0.006 \leq z < 0.012$		730
	$0.012 \leq z < 0.018$		2221
	$0.018 \leq z < 0.024$		7331
for Fig. 4	$0.006 \leq z < 0.012$	$-17 < M_r \leq -15$	1387
		$-19 < M_r \leq -17$	585
		$-22 < M_r \leq -19$	145
for Fig. 5	$0.012 \leq z < 0.018$	$-17 < M_r \leq -16$	1425
		$-19 < M_r \leq -17$	1575
		$-22 < M_r \leq -19$	646
for Fig. 7	$0.006 \leq z < 0.012$	$-17 \leq M_r,\ M_g - M_r > 0.60$ (red)	339
		$-17 \leq M_r,\ M_g - M_r \leq 0.60$ (blue)	391
for Fig. 8	$0.012 \leq z < 0.018$	$-17 \leq M_r,\ M_g - M_r > 0.60$ (red)	1071
		$-17 \leq M_r,\ M_g - M_r \leq 0.60$ (blue)	1150

Table 1. Numbers of galaxies used in calculations of cross-correlation functions.

events with energies beyond 10^{20} eV, are shown as blue circles. The numbers of galaxies we used are summarized in Table 1. We can see that the distribution of galaxies is highly structured. For instance, Virgo cluster is seen at the center of the top panel. Any AGASA event does not spatially correlate with the positions of Virgo cluster, as seen in our previous works [7], which is the same situation as the PAO events [27]. Also, we can find Coma cluster at the center of the bottom left panel and the AGASA event neither correlates with Coma cluster. However, we see that many event correlates with filamentary structures of galaxies by eye. This may be quantified by the cross-correlation function.

The right panels of Fig. 3 are the cross-correlation functions between the AGASA events and the positions of galaxies shown in the corresponding left panels (*histograms*). In order to compare them to the cases of isotropic events, we also show the cross-correlation functions between isotropically distributed events and the galaxies in green. We simulate isotropically distributed events with the same number as the AGASA data 100 times and estimate the averages (*crosses*) and standard deviations of the cross-correlation functions (*error bars*). These standard deviations can be regarded as 1 σ statistical errors.

In the top panel, there is no signal indicating a positive correlation and the signal is consistent with isotropic events, which reflects the fact that the AGASA events do not correlate with not only Virgo cluster but also with the other structures in the nearest Universe. Since the deflections of HECRs from nearby sources are expected to be small, there might not be HECR sources in the Universe within $\sim$ 25 Mpc in the northern sky. In intermediate redshift ranges, which are $0.006 \leq z < 0.012$,

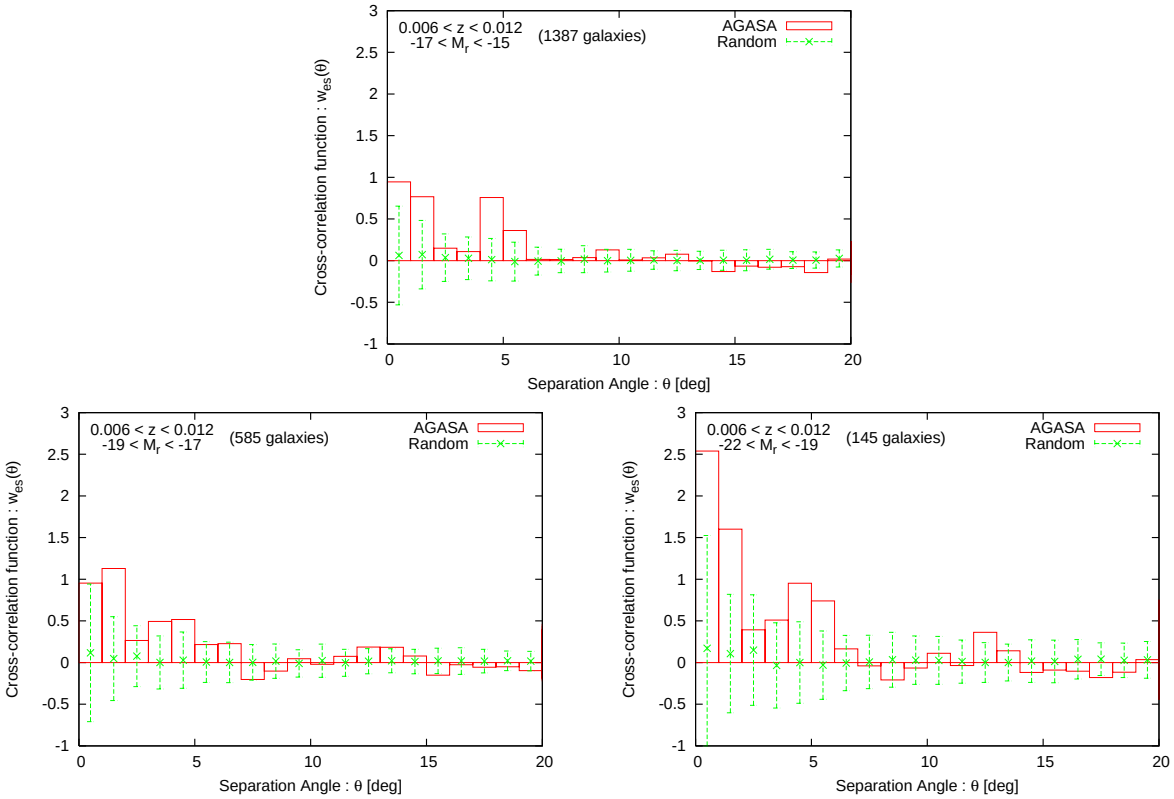

Figure 4. Dependence of the cross-correlation on the r-band absolute magnitude of SDSS galaxies with the redshift of 0.006-0.012.

$0.012 \leq z < 0.018$, we can find positive signals within $\sim 5°$. These reflect about 10 events seen to correlate with filamentary structures of galaxies. These correlations are similar to the PAO results in Ref. [2, 3] because a large fraction of the PAO-correlated AGNs, which are a representative of large-scale structure of local Universe, is distributed at around $z \sim 0.01$, which corresponds to ~ 50 Mpc [28]. Also, local Universe with such a size may have a volume enough to contain HECR sources and the deflections of UHECR trajectories may not be critical. Thus, we can interpret these positive signals as the appearance of HECR sources. Under this interpretation, the angular scale of the positive correlations corresponds to the maximum value of HECR deflections in the local Universe. Finally, positive correlation is not found in the bottom panel. Large deflections of HECRs due to their large propagation distance might let correlation disappear.

3.2. Dependence on Absolute Magnitude

In the previous section, we found the positive correlation between the AGASA events and SDSS galaxies within $0.006 \leq z < 0.012$ and $0.012 \leq z < 0.018$. In this section, we focus on galaxies in these redshift ranges and investigate the dependence of the cross-correlation signals on their r-band absolute magnitude.

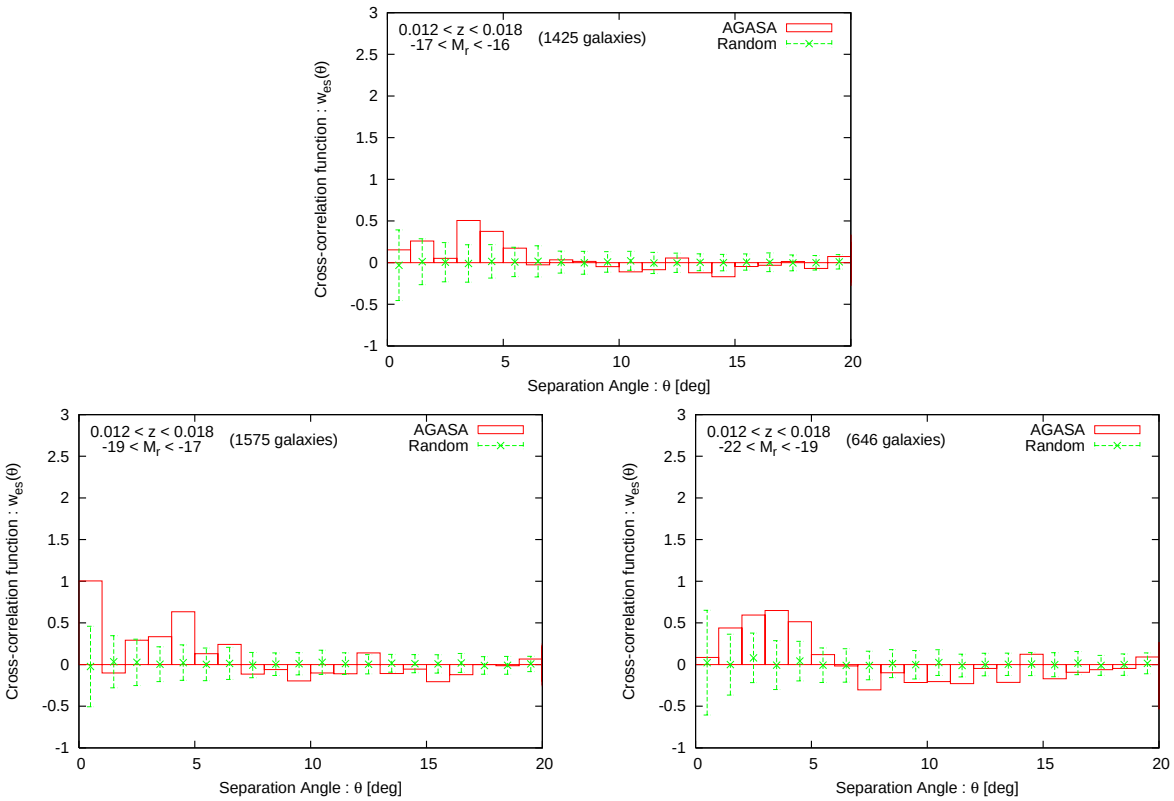

Figure 5. Same as Fig. 4, but the redshift range of galaxies is $0.012 \leq z < 0.018$.

Fig. 4 shows the cross-correlation functions of the AGASA data and SDSS galaxies with $0.006 \leq z < 0.012$ in several ranges of their r-band absolute magnitude. Although SDSS galaxies with $M_r \leq -17.0$ are taken into account for a volume-limited sample in Section 3.1, we also consider galaxies with $-17.0 < M_r \leq -15.0$ here (*upper panel*) to investigate the correlation with faint galaxies. Note that $M_r = -15.0$ is smaller than the flux limited by $m_r = 17.6$ and therefore these galaxies are completed in this redshift range (see Fig. 1). The lower panels show the cross-correlation functions with galaxies with $-19.0 < M_r \leq -17.0$ and $M_r \leq -19.0$ as histograms. We also show the cross-correlation functions with the galaxies and isotropic HECR distribution with 57 events, and their standard deviations ($\sim 1\sigma$ statistical errors), as for Fig. 3. We can find the strongest positive signal at the angular scale within $\sim 5^\circ$ in the 3 panels in the lower right panel. Although the number of galaxies in this M_r range is only 145, we can see such strong signals against a simulation by isotropic events. This implies that the AGASA events were generated in the luminous (generally large) galaxies or at least in an environment where there is a number of luminous galaxies.

Fig. 5 shows the same as Fig. 4, but the redshift range considered is $0.012 \leq z < 0.018$. Since the r-band absolute magnitude corresponding to the limited flux is smaller than in $0.006 \leq z < 0.012$, we do not consider an absolute magnitude range of $-17.0 < M_r \leq -15.0$. Instead of this, we consider galaxies with $-17.0 < M_r \leq -16.0$

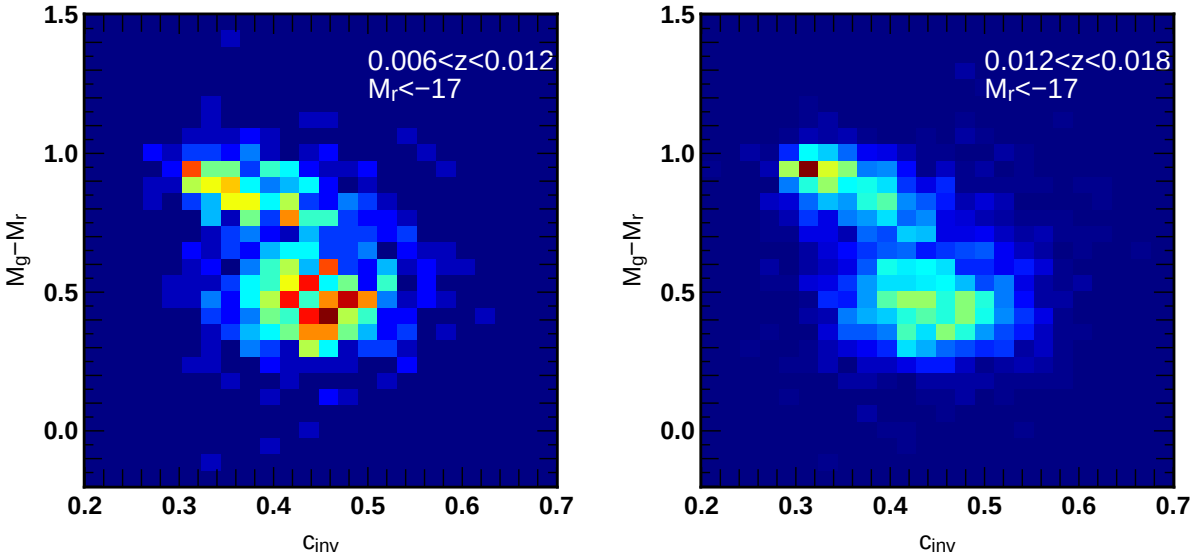

Figure 6. Numbers of SDSS galaxies with the redshifts of $0.006 \leq z < 0.012$ (*left*) and $0.012 \leq z < 0.018$ (*right*) as a function of a concentration parameter, $c_{\rm inv}$, and the difference of absolute magnitude at g-band and r-band. The numbers increase with approaching red from blue.

for fainter galaxies. We cannot find clear difference like Fig. 4 among the 3 ranges of absolute magnitude. Reasons might be a smaller flux of HECRs for each source and larger deflection angles of their propagating trajectories due to source distances larger than the case of Fig. 4. In order to investigate whether the same trend as in Fig. 4 is realized in this redshift range or not, we need more number of HECR events.

3.3. Dependence on Color and Morphology

The color of a galaxy reflects the population of stars in the galaxy and therefore the evolution history of the galaxy. Thus, the dependence of HECR-galaxy correlation on the color of galaxies informs us of the epochs of HECR generation in the history of galaxies and environment around HECR sources. This can be a hint to constrain the sources of HECRs.

Colors of galaxies are generally defined as difference between magnitudes in two different bands in astronomy, and therefore the definition of colors is not unique. Here, we define the colors of galaxies as $M_g - M_r$, which is difference between g-band and r-band absolute magnitudes. Since the wavelength of the r-band is larger than g-band, a galaxy with large $M_g - M_r$ is called relatively red and vice versa. $M_g - M_r$ is a good indicator of contents of galaxies because the $4000\mathring{A}$ break of galaxies is included in g-band. This break is the appearance of long-lived stars like K-type stars. Thus, strong star forming and a number of young (massive) stars are not expected in galaxies with a strong spectral break at $\sim 4000\mathring{A}$, i.e. relatively red galaxies for the color definition.

The morphologies of galaxies also have information on objects in the galaxies.

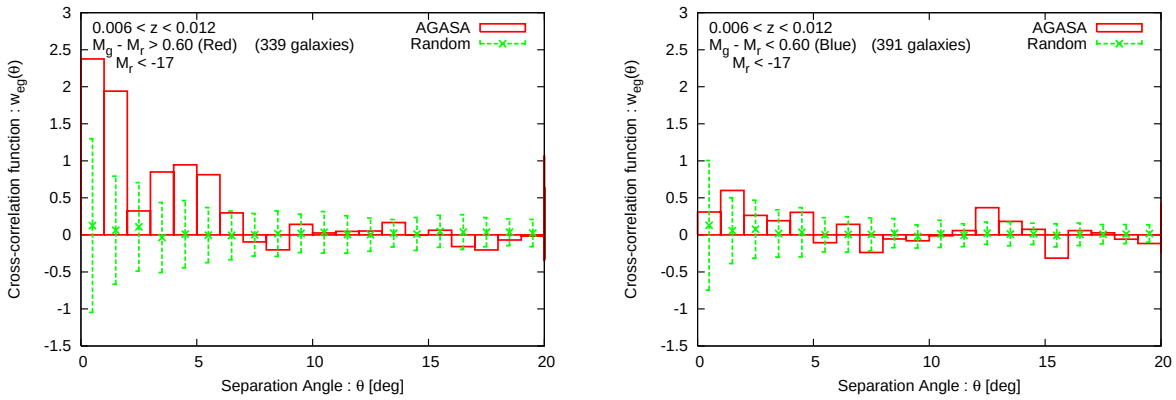

Figure 7. Dependence of the cross-correlation on the color of SDSS galaxies with the redshift of 0.006-0.012.

Galaxies accompanying strong non-thermal radio emission, like radio galaxies, have a tendency to be early-type (elliptical) morphology [29]. On the other hand, several works have pointed out that the host galaxies of γ-ray bursts (GRBs) might have late-type (like irregular or spiral) morphology [30, 31]. The NYU-VAGC attaches the ratio of two Petrosian radii $c_{\rm inv} = r_{50}/r_{90}$ called a (inverse) concentration index. This index is a good indicator to the morphological type of each galaxy [32]. Since elliptical galaxies tend to fade out slowly with the distance from the center, they have relatively smaller concentration indices. On the other hand, late-type galaxies have large concentration indices. Ref. [32] compared concentration indice with morphologies of SDSS galaxies with their apparent magnitude above 16.0 detected during a commissioning phase and found that the best criterion between early-type and late-type morphologies is $c_{\rm inv} \sim 0.35$.

Fig. 6 shows the frequency distributions of galaxies with $M_r \leq -17$ and the redshift ranges of $0.006 \leq z < 0.012$ (*left*) and $0.012 \leq z < 0.018$ (*right*) on a parameter space of $c_{\rm inv}$ and $M_g - M_r$. The number of galaxies increases when the color in each cell is close to red. In both panels, the distribution of galaxies can be separated above and below $M_g - M_r \sim 0.6$. Thus, we define galaxies with $M_g - M_r$ above and below 0.6 as red and blue galaxies in this study, respectively. On the other hand, the distribution cannot be clearly separated in the direction parallel to $c_{\rm inv}$, but a large fraction of the galaxies have $c_{\rm inv} > 0.35$, which means late-type galaxies.

Fig. 7 shows the cross-correlation functions of the AGASA data with SDSS galaxies with $0.006 \leq z < 0.012$ which have $M_g - M_r > 0.6$ (red; *left*) and $M_g - M_r \leq 0.6$ (blue; *right*). We can obviously find that relatively red galaxies strongly correlate with the AGASA events, while the correlation with blue galaxies is consistent with random simulations. This implies that HECRs are generated in red galaxies or at least in an environment in which many relatively red galaxies exist. Since a red galaxy is luminous and thus large because it is after many stars are made, this result is consistent with that in the previous section. Such a feature is not clear for galaxies with $0.012 \leq z < 0.018$

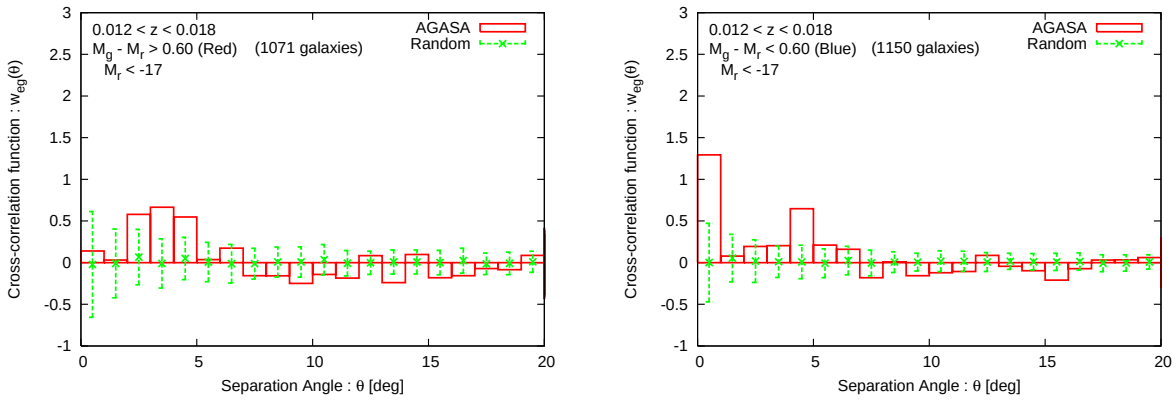

Figure 8. Same as Fig. 7, but the redshift range of galaxies is $0.012 \leq z < 0.018$.

as seen in Fig. 8.

We specially focus on galaxies with $M_r \leq -19$ and $0.006 \leq z < 0.012$, which strongly correlate with the AGASA events. Fig. 9 shows plots of the galaxies on a parameter space of $c_{\rm inv}$ and $M_g - M_r$ (*red*). We also plot galaxies within 5° from any AGASA events in green, whose angular scale reflects the result that the spatial correlation scale is $\sim 5°$ (see Fig. 3). We can find that all the galaxies within 5° from the AGASA events are $M_g - M_r > 0.6$, relatively red, while $c_{\rm inv}$ are broadly distributed. We also check the morphologies of these galaxies (*green points*) by eye by using SDSS DR7 navigate tool [33]. 2 galaxies with $c_{\rm inv} < 0.35$ are elliptical, but the other have late-type morphologies.

In the summary of this section, we found that the AGASA events significantly correlate with SDSS galaxies with $0.006 \leq z < 0.012$ and $0.012 \leq z < 0.018$ within the angular scale of $\sim 5°$. Especially in the case of $0.006 \leq z < 0.012$, the correlation tended to be stronger for luminous ($M_r < -19$) and red galaxies. The luminous galaxies around the AGASA events were relatively red and morphologically late-type. For $0.012 \leq z < 0.018$, the dependence of the correlation on colors and morphologies of galaxies was not clear. This was possible because the flux of HECRs from a sources with this redshift range is smaller than for $0.006 \leq z < 0.012$ and/or the trajectories of HECRs are more deflected than for sources with $0.006 \leq z < 0.012$. These dependencies should be tested in the future when the more number of HECR events are accumulated.

4. Discussion

In this section, we discuss the sources of HECRs based on results found in Section 3. We specially focus on the results on galaxies with $0.006 \leq z < 0.012$, though it is non-trivial that the correlation features in $0.006 \leq z < 0.012$ are universal. Potential sources of HECRs ever proposed are GRBs [34, 35, 36], newly born magnetars [37], radio-loud active galactic nuclei (AGNs) [38, 39, 40], and clusters of galaxies [41, 42]. We discuss the relations between our results and the features of the host galaxies of GRBs (Section

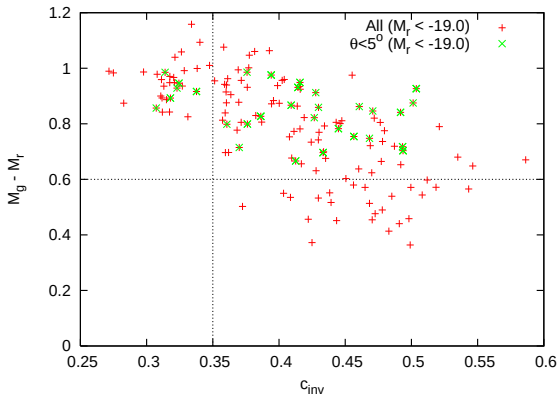

Figure 9. Distribution of galaxies with $0.006 \leq z < 0.012$ and $M_r \leq -19$ on a $c_{\rm inv}$-$M_g - M_r$ plane. The red crosses are all the galaxies and the green circles are galaxies which are placed within 5° from the AGASA events.

4.1), magnetars (Section 4.2), and AGNs (Section 4.3) under the assumption that the observed correlation is true correlation between HECRs and their sources. The case of clusters of galaxies is not discussed. In Section 4.4, we refer to the possibility that the correlation is *fake* due to the propagation of HECRs in magnetized intergalactic space for completeness. Finally, we discuss a constraint on Galactic Magnetic Field (GMF) from the results in this study in Section 4.5.

4.1. γ-ray Bursts

Since GRBs (at least long-duration ones) are thought to be related to explosions of massive stars at the end of their life [43, 44, 45], their host galaxies are expected to have high star formation rate. Although the GRB population with redshift is small, many observations have indicated that the typical nature of GRB host galaxies is, in fact, of faint star-forming galaxies dominated by a young stellar population [46]. In general, the host galaxies have low luminosities [30], low masses [31], and therefore low metallicities [47, 48].

Although the host galaxies are too faint to be observed by galaxy surveys, it is no problem in local Universe where we consider because the absolute magnitudes of galaxies observed in the local Universe are comparable with those of GRB host galaxies observed in high redshift Universe. Fig.6 of Ref. [31] gave the histogram of the number of GRB host galaxies as a function of B-band (centered at 442 nm) absolute magnitude. Almost all of GRB host galaxies have $-22 < M_B \leq -17$. This has been unchanged in a recent larger database [49] Since a large fraction of SDSS galaxies has $M_g - M_r > 0$, GRB host galaxies are expected to be more luminous in r-band than B-band. Note that the central wavelengths of g-band and r-band are 477.0 nm close to B-band and 623.1 nm, respectively. Thus, our approximately volume-limited sample of galaxies, which consists of galaxies with $M_r \leq -17$, includes GRB host candidates. We can directly compare our results with the features of GRB host galaxies.

The color of GRB host galaxies tends to be blue [31] even in nearby Universe [50]. We should notice the definition of the color of galaxies. In Ref. [31], the authors discussed the colors of GRB host galaxies by using infrared wavelengths, $R-K$, which is different from the definition in this study. However, the essence of both definitions is the same, i.e. these are indicators of old (long-lived) star population, and therefore we can compare results of this study with those of GRB host studies qualitatively. It might be difficult that GRBs are HECR sources from the qualitative discussion, since the AGASA events correlate with relatively red galaxies. Of course, qualitative discussion should be performed under the same definition of galaxy colors.

Since GRBs are transient phenomena, we must consider the time-delay of HECRs in intergalactic space and it should be compared with the typical lifetime of massive stars as progenitors of GRBs. If the typical time-delay of HECRs is larger than the lifetime of massive stars, galaxies which correlate with the AGASA events do not seem to be blue. Although the masses of GRB progenitors have uncertainty, the masses are larger than $\sim 25M_{\odot}$ or typically $\sim 40M_{\odot}$ under a collapser model [51] in which requires black hole formation by stellar core collapse. A typical main sequence lifetime is $\sim 10^7$ yrs. Several IGMF models predict that a fraction of HECRs has time-delay larger than $\sim 10^7$ yrs even for protons [52, 53] However, the trajectories of such HECRs are highly deflected and the correlation between HECRs and the positions of their sources is lost. The correlation with matter distribution can be observed, but it is *fake* correlation with their true sources [54] (see Section 4.4 in detail). In this case, it is difficult to confirm GRB origin of HECRs from information on colors of the correlated galaxies. Note that other IGMF models predict much smaller time-delay [55, 56]. If such a small IGMF is realized in the Universe, the discussion on colors of the correlated galaxies above is allowed.

GRB host galaxies are morphologically irregular or late-type [31]. In our study, Fig. 6 shows that a large fraction of galaxies has $c_{\rm inv} > 0.35$, which means they are late-type galaxies. The completeness of the division is $\sim 90\%$ [32]. Thus, GRB origin of HECRs is not inconsistent with the results of the analyses. Note that a recent study which use the largest sample of GRB host galaxies reports no compelling evidence that GRB host galaxies are peculiar galaxies in the point of their morphologies [49]. Thus, unfortunatly it is not clear from the results of this study whether GRBs are HECR sources or not.

4.2. Magnetars

Magnetars are thought to be neutron stars with extremely strong magnetic fields ($\sim 10^{15-16}$ G), but their production mechanism is still controversial (see [57] for a review). Although we know about ten of magnetar candidates, the positions of a large fraction of magnetars are associated with supernova remnants or massive stellar cluster [58]. This indicates that magnetars are produced through core-collapse of massive stars like GRBs. Observationally, GRB060218 (sometimes categolized into X-ray flush) was a possible candidate of a GRB leaving a magnetar [59] and its progentor mass was

estimated as $\sim 20 M_{\odot}$, relatively smaller than the masses of typical GRB progenitors. Also, it was theoretically proposed that a class of GRBs, called low-luminosity GRBs, accompany the production of magnetars [60].

The nature of the host galaxies of magnetars is poorly known because almost all the magenetar candidates are located in our Galaxy. One of the 2 exceptions is in Large Magellanic Cloud (SGR 0526-66) [61] and the other is in Small Magellanic Cloud (CXOU J0100-72) [62]. Therefore, there is little information on host galaxies other than our Galaxy. However, based on a hypothesis that magnetars are created by core-collapse of massive stars as discussed above, they are more frequently produced in star-forming galaxies, similar to the case of GRBs, but a little redder galaxies are allowed because the masses of magnetar progenitors are thought to be smaller than those of GRBs. Thus, the constraints may match the possible conditions of the host galaxies of magnetars a bit better than for GRBs.

4.3. Active galactic nuclei

Many models to accelerate particles to the highest energies at AGNs have been proposed: at giant radio lobes of Fanaroff-Reily II (FRII) galaxies with Mpc-scale jets [38], giant flares of blazars [40], and the shocks of cocoon expansion of small version ($\sim$ 1 kpc) of radio-loud galaxies [39]. An important point is that all of these scenarios requires galaxies dominated by non-thermal radiation, which have generally early-type morphologies [29], though their required sizes of sources are different. On the other hand, a large fraction of SDSS luminous galaxies with $0.006 \leq z < 0.012$ has late-type morphologies. Thus, it might be difficult that these source candidates are HECR sources.

4.4. Propagation effects

In the 3 previous sections, we treat the cross-correlation between HECRs and their sources as true one. However, the arrival directions of HECRs can be far from the positions of HECR sources without reducing the correlation with matter distribution, if IGMF is strong. Note that IGMF strength and structures are still under debate.

Ref. [63] pointed out the possibility of *fake* correlation. In this scenario, even the HECRs are scattered by strongly magnetized structure of the Universe called scattering centers like clusters of galaxies, large magnetized lobes of radio galaxies and so on. Therefore, if there is a real source of HECRs far from a region which observed HECRs correlate with, the HECRs seems to come from the region when the HECRs are scattered by a strong magnetic field in the region. Ref. [63] reported that about 50% of the PAO events published in Ref. [3] could be such fake correlation. A similar phenomena is observed in Ref. [54] by simulations of propagation of protons considering a sophisticated and simulated IGMF model [53]. They also show that predicted angles between the arrival directions of HE protons and AGN-like objects defined in their simulations are consistent with the correlation angles derived by the PAO [3] even if there are real

sources far from the AGN-like objects. In any case, regions which correlate with the HE events could not always point out real sources. We should keep it in mind that there are much uncertainty on IGMF modelling. There are also IGMF models to predict smaller deflections of HECRs [55, 56].

4.5. Constraint on GMF

The angular scale of the positive correlation enables us to constrain intervening magnetic fields, especially Galactic magnetic field (GMF). Since the structure of GMF is independent of galaxy distribution in local Universe, GMF can reduce the expected spatial correlation between the arrival directions of HECRs and the positions of nearby galaxies if GMF largely deflects HECR trajectories. However, we found the correlation of HECRs and large-scale structure of matter distribution. Thus, GMF is not too large to weaken such correlation.

Moreover, we can constrain GMF structure from the results of this study under the assumption that the observed correlation is true correlation between HECRs and their sources, because the spatial correlation is sensitive to GMF models in the northern sky [64, 65]. Refs. [64, 65] investigated the correlation between HE protons and their sources taking their deflections by several GMF models into account. The angular scale of positive correlation which we found in Section 3 was estimated as $\sim 5^\circ$. This is comparable with the angular scale of positive correlation with HECR sources expected by bisymmetric spiral GMF models predicted in those works. Although axisymmetric GMF models predicted cross-correlation functions consistent with isotropically distributed HE protons within error bars, this does not reject the possibility of the axisymmetric GMF models. However, protons with energies of $10^{19.8}$ eV are deflected by more than 5° in about a half of the northern sky for the axisymmetric GMF models. Thus, it might be difficult that the axisymmetric models are realized, i.e., there might be reversals of GMF at least outside the solar system. Furthermore, the small deflection implies proton-dominated composition of HECRs.

We should notice 2 limitations on the discussion above. One is that the SDSS surveys about a half of the northern sky. The discussion above is based on the cross-correlation between HECRs and galaxies in a sky where the SDSS observed. The other is the definition of the angular scale for positive correlation in this study. That angular scale is determined as angular scale in which correlation signals exceed to the 1 σ error bars attached into the cross-correlation function calculated from random event distribution. When the number of observed events increases, the error bars decrease and the angular scale of the positive correlation might be larger.

5. Conclusion

In this study, we investigated the correlation between the arrival directions of HECRs detected in the northern sky (the AGASA data) and galaxy distribution observed by

the SDSS. The SDSS can observe faint galaxies, and therefore SDSS galaxies are a good sample to investigate the correlation with the large-scale structure of matter in local Universe. We found the positive correlation of the AGASA events with SDSS galaxies within the angular scale of $\sim 5^\circ$ with the redshift ranges of $0.006 \leq z < 0.012$ and $0.012 \leq z < 0.018$ for the first time. This result supported a hypothesis that the sources of HECRs are related to galaxy distribution even in the northern sky, which has been already indicated by several analyses of the PAO data in the southern sky [2, 3, 4, 5, 6, 7]. We also tested the dependencies of the correlation signals on the r-band absolute magnitude, color, and morphology of the galaxies, since these information is generally useful to constrain HECR sources involved in the host galaxies. For galaxies with $0.006 \leq z < 0.012$, we found that the AGASA events correlated with luminous ($M_r \leq -19$) and red ($M_g - M_r > 0.6$) galaxies, and the luminous galaxies around the AGASA events were relatively red and morphologically late-type. Such dependencies were not clear for galaxies with $0.012 \leq z < 0.018$. This was possible because the flux of HECRs from a sources with this redshift range is smaller than for $0.006 \leq z < 0.012$ and/or the trajectories of HECRs are more deflected than for sources with $0.006 \leq z < 0.012$.

We discussed possible source candidates based on our results for galaxies with $0.006 \leq z < 0.012$ in Section 4. Unfortunately, the interpretation of the results is ambiguous at present because of uncertainty of relations between HECR source candidates and the nature of their host galaxies, and our poor knowledge on intervening magnetic fields. Under the limitations, possible interpretation is summarized as follows: Morphology dependence of galaxies correlating with the AGASA events is positive for GRBs and magnetars, but the colors of these galaxies are relatively red, contrary to relatively blue colors expected for these objects. Note that the discussion on the colors was only qualitative. More detail and quantitative discussion is required to confirm/reject GRB or magnetar origin of HECRs. On the other hand, HECR generation by non-thermal phenomena related to AGNs might be difficult from results in this study because the morphologies of luminous galaxies near the AGASA events are relatively late-type, though such phonomena are strongly related to galaxies with early-type galaxies.

The interpretation above is based on the assumption that the trajectories of HECRs are not largely deflected by IGMF. When IGMF is strong, fake correlation could occur [63, 54]. The correlation between the arrival directions of HECRs and the positions of their sources is reduced, though the correlation with matter distribution is conserved. In this case, it is not possible to confirm HECR sources by the nature of galaxies correlating with HECR events.

The angular scale of the positive correlation enabled us to constrain intervening magnetic fields under the assumption that we see the correlation between HE protons and their sources. The angular scale estimated in this study, $< 5^\circ$, was compared with theoretical predictions by Ref. [65]. The angular scale was consistent with predictions based on bisymmetric spiral field models of GMF. Since the larger angular deflections of

HE protons are predicted for axisymmetric GMF models, it might be difficult to realize the axisymmertic models.

In order to investigate correlation signals between HECRs and matter distribution/their sources more accurately, we need more number of HECR events. It was not clear whether the correlation features found in this study for galaxies with $0.006 \leq z < 0.012$ are common in the Universe. This can be checked by increasing the observed number of HECRs. We can also understand intervening magnetic fields and the nature of HECR sources. Ref. [66] predicted the spatial correlation between HE protons and their sources in local Universe even taking a realistically structured IGMF model into account, which was clearly visible by accumulating ~ 200 events above $\sim 6 \times 10^{19}$ eV for the number density of HECR sources of 10^{-5} Mpc^{-3}. Data accumulation in the northern sky is in progress. The total exposure of the Telescope Array have already reached 75% of the AGASA exposure [67] and is expected to reach that of the AGASA in this year. Thus, their data is quite useful to test the correlation and the nature of the host galaxies of HECR sources. Also, two projected HECR observatories with extremely large effective area, Extreme Universe Space Telescope (JEM-EUSO) [68] and the northern site of the PAO [69], enable us not only to clarify the correlation but also to unveil the positions of HECR sources in the northern sky of local Universe.

Acknowledgments

We are grateful to K.Maeda and I.Kayo for useful discussion. This work is supported by Grants-in-Aid for Scientific Research from the Ministry of Education, Culture, Sports, Science and Technology (MEXT) of Japan through No.21840019 (H.T.) and No.19104006 (K.S.). The work of T.N. is supported by the JSPS fellow. This work is also supported by World Premier International Research Center Initiative (WPI Initiative), from the MEXT of Japan.

Funding for the SDSS and SDSS-II has been provided by the Alfred P. Sloan Foundation, the Participating Institutions, the National Science Foundation, the U.S. Department of Energy, the National Aeronautics and Space Administration, the Japanese Monbukagakusho, the Max Planck Society, and the Higher Education Funding Council for England. The SDSS Web Site is http://www.sdss.org/.

The SDSS is managed by the Astrophysical Research Consortium for the Participating Institutions. The Participating Institutions are the American Museum of Natural History, Astrophysical Institute Potsdam, University of Basel, University of Cambridge, Case Western Reserve University, University of Chicago, Drexel University, Fermilab, the Institute for Advanced Study, the Japan Participation Group, Johns Hopkins University, the Joint Institute for Nuclear Astrophysics, the Kavli Institute for Particle Astrophysics and Cosmology, the Korean Scientist Group, the Chinese Academy of Sciences (LAMOST), Los Alamos National Laboratory, the Max-Planck-Institute for Astronomy (MPIA), the Max-Planck-Institute for Astrophysics (MPA), New Mexico State University, Ohio State University, University of Pittsburgh, University

of Portsmouth, Princeton University, the United States Naval Observatory, and the University of Washington.

[1] Takeda M *et al* 1999 *Astrophys. J.* **522** 225
[2] Abraham J *et al* 2007 *Science* **318** 938
[3] Abraham J *et al* 2008 *Astropart. Phys.* **29** 188
[4] Kashti T, Waxman E 2008 *JCAP* **05** 006
[5] George M *et al* 2008 *MNRAS* **388** L59
[6] Ghisellini G *et al* 2008 *MNRAS* **390** L88
[7] Takami H *et al* 2009 *JCAP* **06** 031
[8] Hague J D *et al* 2009 *Proc. 31th Int. Cos. Ray. Conf.* #143
[9] Aublin J *et al* 2009 *Proc. 31th Int. Cos. Ray. Conf.* #491
[10] Stanev T 1995 *Phys. Rev. Lett.* **75** 3056
[11] Uchihori Y 2000 *Astropart. Phys.* **13** 151
[12] Saunders W 2000 *MNRAS* **317** 55
[13] York D *et al* 2000 *Astron. J.* **120** 1579
[14] Hayashida N *et al* 2000 *Astron. J.* **120** 2190
[15] Takeda M *et al* 1998 *Phys. Rev. Lett.* **81** 1163
[16] Greisen K 1966 *Phys. Rev. Lett.* **16** 748
[17] Zatsepin G & Kuz'min V 1966 *JETP Lett.* **4** 78
[18] Bhattacharjee P & Sigl G 2000 *Phys. Rep.* **327** 109
[19] Abbasi R *et al* 2008 *Phys. Rev. Lett.* **100** 101101
[20] Abraham J *et al* 2008 *Phys. Rev. Lett.* **101** 061101
[21] Abazajian K N *et al* 2009 *Astrophys. J. Suppl.* **182** 543
[22] Blanton M *et al* 2005 *Astron. J.* **129** 2562
[23] Blake C *et al* 2006 *MNRAS* **368** 732
[24] Sommers P 2001 *Astropart. Phys.* **14** 271
[25] Hamilton A J S & Tegmark M 2004 *MNRAS* **349** 115
[26] Swanson M E C *et al* 2008 *MNRAS* **387** 1391
[27] Gorbunov D *et al* , 2008 *JETP Lett.* **87** 461
[28] Zaw I, Farrar G R, Greene J E 2009 *Astrophys. J.* **696** 1218
[29] Krolik J H 2000 *Active Galactic Nuclei*, Princeton University Press
[30] Fruchter A S *et al* 1999 *Astrophys. J. Lett.* **519** L13
[31] Le Floc'h E *et al* 2003 *Astron. & Astrophys.* **400** 499
[32] Shimasaku K *et al* 2001 *Astrophys. J.* **122** 1238
[33] SDSS Data Release 7 Navigate Tool http://cas.sdss.org/astro/en/tools/chart/navi
[34] Waxman E 1995 *Phys. Rev. Lett.* **75** 386
[35] Vietri M 1995 *Astrophys. J.* **453** 883
[36] Murase K 2006 *Astrophys. J. Lett.* **651** L5
[37] Arons J 2003 *Astrophys. J.* **589** 871
[38] Rachen J, Biermann P 1993 *Astron. & Astrophys.* **272** 161
[39] Berezhko E 2008 *Astrophys. J. Lett.* **684** L69
[40] Farrar G, Gruzinov A 2009 *Astrophys. J.* **693** 329
[41] Kang H, Rachen J, Biermann P 1997 *MNRAS* **286** 257
[42] Inoue S *et al* 2007 *Proc. 30th Int. Cos. Ray. Conf. (Merida)* **4** 555
[43] Galama T J *et al* 1998 *Nature* **395** 670
[44] Hjorth J *et al* 2003 *Nature* **423** 847
[45] Stanek K Z *et al* 2003 *Astrophys. J. Lett.* **591** L17
[46] Christensen L, Hjorth J, Gorosabel J 2004 *Astron. & Astrophys. 425* 913
[47] Gorosabel J *et al* 2005 *Astron. & Astrophys.* **444** 711
[48] Wiersema K *et al* 2007 *Astron. & Astrophys.* **464** 529
[49] Savaglio S, Glazebrook K, Le Borgne D 2009 *Astrophys. J.* **691** 182
[50] Sollerman J 2005 *New Astron.* **11** 103
[51] Woosley S E 1993 *Astrophys. J.* **405** 273

[52] Sigl G, Miniati F, Ensslin T.A. 2004 *Phys. Rev.* **D70** 043007
[53] Das S *et al* 2008 *Astrophys. J.* **682** 29
[54] Ryu D, Kang H, Das S 2009 *Proc. 31th Int. Cos.Ray Conf. (Lodz)* #839
[55] Dolag K *et al* 2005 *JCAP* **01** 009
[56] Takami H, Yoshiguchi H, Sato K 2006 *Astrophys. J.* **639** 803 (Erratum 2006 *ibid.* **653** 1583
[57] Mereghetti S 2008 *Astron. Astrophys. Rev. 15* 225
[58] Gaensler B M *et al* 2001 *Astrophys. J.* **559** 963
[59] Mazzali P A *et al* 2006 *Nature* **442** 1018
[60] Toma K *et al* 2007 *Astrophys. J.* **659** 1420
[61] Cline T L *et al* 1980 *Astrophys. J. Lett.* **237** 1
[62] Lamb R C *et al* 2002 *Astrophys. J. Lett.* **574** L29
[63] Kotera K, Lemoine M 2008 *Phys. Rev.* **D77** 123003
[64] Takami H, Sato K 2009 *Proc. 31th Int. Cos. Ray Conf. (Lodz)* #888
[65] Takami H, Sato K 2009 *Preprint* arXiv:0909.1532
[66] Takami H, Sato K 2008 *Astrophys. J.* **678** 606
[67] Taketa A *et al* 2009 *Proc. 31th Int. Cos. Ray Conf. (Lodz)* #0855
[68] Ebisuzaki T. *et al* 2009 *Proc. 31th Int. Cos. Ray Conf. (Lodz)* #1035
[69] Harton J. *et al* 2009 *Proc. 31th Int. Cos. Ray conf. (Lodz)* #458